Exploration of using a pressure sensitive mat for respiration rate and heart rate estimation*

Wenjun Huang[1], Murtaza Bulut[2], Ron van Lieshout[2], and Kiran Dellimore[2], *Senior Member, IEEE*

Abstract— Measuring the respiration and heart rate unobtrusively in home settings is an important goal for health monitoring. In this work, use of a pressure sensitive mat was explored. Two methods using body morphology information, based on shoulder blades and weighted centroid, were developed for respiration rate (RR) calculation. Heart rate (HR) was calculated by combining the frequency information from different body regions. Experimental data were collected from 15 participants in a supine position via a pressure sensitive mat placed under the upper torso. RR and HR estimations derived from accelerometer sensors attached to participants' bodies were used as references to evaluate the accuracy of the proposed methods. All three methods achieved a reasonable estimation compared to the reference. The root mean squared error of the proposed RR estimation methods were 1.32 and 0.87 breath/minute respectively, and the root mean squared error of the HR estimation method was 5.55 bpm.

I. INTRODUCTION

Physiological parameters such as heart rate (HR), respiration rate (RR), blood pressure, and body temperature are indicators of the health status of an individual. Among these vital signs, RR and HR are the most important since significant changes in these parameters can be strong predictors of adverse events such as cardiac arrest, stroke and unplanned intensive care unit admission [1]. Since many adverse cardiovascular and respiratory events can occur outside of clinical settings, and in particular during sleep [2], it is desirable to be able to monitor the vital signs of at-risk individuals when they are in a lying position. Conventional techniques for RR and HR measurement, based on skin contacting electrodes placed at the chest or abdomen [3], can be obtrusive and unsuitable for long-term monitoring outside clinical settings [4]. As a result, in recent years, unobtrusive monitoring approaches based on ballistocardiography, laser, camera, radio, and ultrasound have increasingly been explored.

Pressure sensitive mats (PSMs) are among the many different unobtrusive monitoring techniques which have been investigated. To date, previous RR estimation studies on PSMs have been based on analysis of one-dimensional signals derived from the PSM and therefore did not account for spatial variations in signal intensity, which may impact robustness and reliability. Moreover, robust HR estimation from PSMs is challenging because the power of the heartbeat

signal is much lower that of the breathing signal. This means that it has an inherently lower signal-to-noise ratio (SNR).

In this paper, we explore new methods to continuously and robustly estimate the RR and HR of individuals lying on a PSM. To accomplish this we treat the data collected from the PSM as a two-dimensional signal, emphasizing the region of interest (ROI) positioning and shape variation.

II. EXPERIMENTAL SETUP

Data were collected from 15 adult participants (9 males and 6 females). The median of the participants' age and BMI are 37 and 25.8 respectively. During the tests, participants were asked to lie stationary in a supine position. In addition, the participants were asked to maintain normal breathing during the 3-minute long measurement. The sensor used for data acquisition was the CONFORMat system (Tekscan Inc., Boston MA, USA) which is a bi-dimensional pressure-mapping sensor, that was placed under the upper torso. Tekscan contains a 42×48 array of discrete pressure sensors whose signals are quantified on a scale from 0 to 255 with a sampling rate of 50 Hz. A detailed description of the experimental protocol can be found in [5]. The Experiment Protocol involving human subjects described in this paper was approved by the Philips Internal Committee for Biomedical Experiments (Reference: ICBE-2-27345).

III. RESPIRATION RATE AND HEART RATE ESTIMATION METHODS

A. Accelerometer reference

In this study, the estimation derived from an accelerometer sensor (LIS344ALH, STMicroelectronics, Geneva, Switzerland) was considered to be a reference to calculate the accuracy of the RR and HR estimation from the PSM. Therefore, a reliable estimation from the accelerometer is very important. The raw signals were extracted from the 3-axes channels of the accelerometers placed on the body. To be specific, the channel chosen for RR was the sum of the three axes of the accelerometer placed on the left lower abdomen. And the channel chosen for HR was the z-axis of the accelerometer placed on the right thigh above the knee. The mentioned sensors locations and channels were selected for their robust and consistent estimation, after careful and detailed analysis of different options. The orientation of the three accelerometers' axes can be found in [5].

Since respiration signal and heartbeat signal are nonstationary, it is necessary to consider both time and frequency

when estimating the RR and HR. Frequently used time-frequency analysis methods are short-time Fourier transform (STFT), continuous wavelet transform (CWT) and synchrosqueezing transform (SST) [6]. Compared with STFT, CWT and SST have higher time domain resolution, which was crucial for our task. However, both CWT and SST were affected by the problem of harmonics. Especially for some participants, the amplitude of the harmonics were similar in magnitude to the fundamental frequency component in the whole measurement. Therefore, we need to distinguish the fundamental frequency component and harmonics through frequency domain analysis. The de-shape synchrosqueezing transform (DSST) uses cepstrum and spectrum to distinguish the fundamental frequency from the harmonics [7]. During the estimation, a 20-second window with a 1-second shift was implemented. All analysis was performed in MATLAB R2020a (MathWorks, Natick MA, USA). A comparison between the results of SST and DSST is shown in Fig. 1. It can be clearly seen that the result of SST (solid line) is influenced by the harmonic of the HR during the measurement while the DSST (dotted line) successfully estimates the fundamental frequency component. Similar results were also obtained for frequencies in the RR range (not shown in the figure).

After implementing DSST, the estimations derived from the accelerometers were post-processed to remove the outlier values which are greater than 1.5 interquartile ranges above the upper quartile or below the lower quartile. For the example output in Fig. 1, the detected outliers are marked with filled circles.
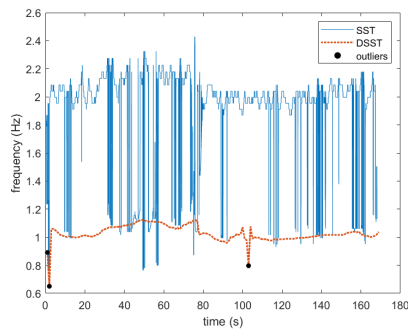
Fig. 1: Comparison between the SST and DSST methods for HR estimation.

B. RR estimation from the PSM based on the ROI (i.e. shoulder-blade based method)

The first method for RR calculation is composed of four main steps: torso segmentation, ROI positioning, signal extraction, and respiration rate estimation.

1) Torso segmentation: Since both the torso and the arms are contained in the raw data (see Fig. 2a), segmenting the torso is helpful in reducing interference. A growth region algorithm was used for segmentation. During segmentation, the seed was set as the location of maximum pressure in the frame. In addition, the centroid of the current segmentation result was stored and compared with the previous one to ensure accuracy. If the distance between two centroids was larger than a prescribed threshold (3 pixels), the current result was rejected. With this computation, the torso contour was successfully found in every frame. The only assumption applied in the segmentation process was that the centroid of the torso in the first frame should approximately be located in the middle of the x-axis. This assumption was consistent with the expected positioning of individuals on the PSM and guaranteed that the segmentation was initiated successfully. An example of a segmentation result is shown in Fig. 2b.
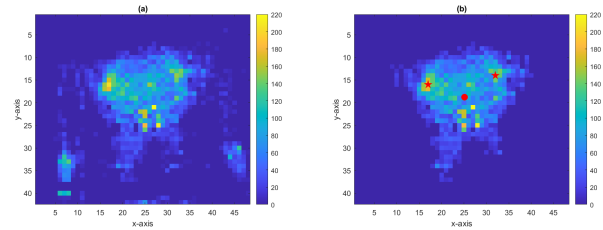
Fig. 2: An example of torso segmentation. (a) Raw frame. (b) Torso segmentation result. The filled stars and circle, mark the locations of the shoulder blades and the weighted centroid, respectively.

2) ROI positioning: We apply a signal extraction method which is distinguished from previously explored approaches since it is focused on the positioning of the ROI based on image analysis. After trying several potential candidates, we noticed that the regions containing the shoulder blades always detected the signal with good quality. Since the regions at the shoulder blades typically had the highest pressure intensity, a 3×3 square average filter was applied on the frame to find the two local maxima in the upper half of the torso (one located on the right half and the other one located on the left half). In addition, a threshold which was defined empirically was introduced to ensure high accuracy in determining the positioning of these two maxima. Since the shoulder blades should roughly be located on the same horizontal line, the positioning result was rejected when the difference between two y-coordinates was larger than a prescribed threshold (3 pixels). The example positioning results are shown in Fig. 2b.

3) Signal extraction: Once the ROI were found, the two-dimensional information was mapped to a one-dimensional signal. All nonzero values in the shoulder blade regions were summed up to obtain the raw signal. This signal was then filtered using a fourth-order Butterworth filter with a passband from 0.08 to 0.67 Hz (corresponding to 5-40 breaths per minute). The Butterworth filter was used to be compliant with the legacy code [5]. In this particular case, the use of the Butterworth filter is not critical, and comparable results are achieved with other types of band-pass filters.

4) Respiration rate estimation: During the estimation of RR, The DSST was also implemented on the filtered signal since the problem of harmonics was again encountered. The window length and the shift of DSST were the same as used in the accelerometer signal estimation.

C. RR estimation from the PSM based on torso-weighted centroid (i.e. weighted-centroid method)

The second method for RR estimation was also based on torso segmentation, therefore the first stage was the same as that described in the previous section. Next, the signal extraction was based on the observation that the vertical movement of the weighted centroid varied according to the inhalation and exhalation. During inhalation, the subject's weighted centroid moves downwards since the lower half of the torso has a better contact with the PSM, while the opposite is true during exhalation. The weighted centroid of the torso was calculated in every frame, and the y-coordinates were sequenced to construct the raw signal. The RR estimation step was the same as the previous method, using DSST to estimate RR while eliminating the influence of harmonics.

D. HR estimation

For the HR estimation, after the torso segmentation, the segmented image was divided into 3 × 3 square blocks. The pixels in each block were summed to construct one-dimensional signals of each 3 × 3 block for the whole 3-minute recording period. Only the signals for the blocks whose percentage of nonzero value was greater than a threshold percentage, defined experimentally, were considered valid. Afterwards, each signal was filtered using a fourth-order Butterworth filter with a passband from 0.67 to 2 Hz (corresponding to 40-120 bpm). Then the STFT with a 20-second window and 1-second shift was implemented on each filtered signal. The reason why the STFT was implemented instead of the DSST was that the filtered signals for HR estimation were barely influenced by the HR harmonics. The maximum frequency, which is the frequency of the highest amplitude point in the frequency spectrum, and the SNR value, which is used as a measure for the prominence of the maximum peak relative to the other peaks, were determined. The SNR was calculated as follows:

$$SNR = \frac{max(peaks)}{\sum peaks} \quad (1)$$

where $peaks$ are the local maxima in the spectrum. An example of the maximum frequencies and the corresponding SNR value is shown in Fig. 3. Each circle represents an estimation for a 3 × 3 block. The x-axis denotes the SNR and the y-axis denotes the maximum frequency.

All valid blocks based frequency calculations were used to generate the final frequency estimation. First, the SNR of each block was mapped to a weight in the range from 0 to 1 using the $softmax$ function. The $softmax$ function is presented below:

$$p(SNR_j) = \frac{exp(SNR_j)}{\sum_{i=1}^{n} exp(SNR_i)} \quad (2)$$

For the final estimation, a sliding window with a width 0.1 Hz moved through the frequency axis, and the weights of the block estimations located in the window were summed up. The frequency band with maximum total weight was selected. The final HR was calculated from the weighted average of the frequencies located in the selected frequency band.
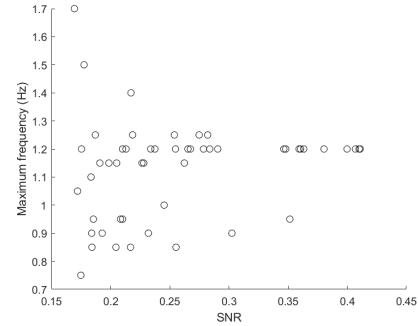
Fig. 3: An example of the maximum frequency and signal to noise ratio (SNR) values calculated for each 3-by-3 block.

IV. RESULTS

The performance of the proposed algorithms was compared to the values calculated from the accelerometer signal. Two 5-second long segments were discarded at the beginning and the end respectively during the data analysis to avoid the interference caused by posture adjustment. TABLE I tabulates the mean for accelerometer estimations, and the difference between the means of the proposed methods estimations and accelerometer estimations. The difference was computed as: $PSM\ based\ estimation - accelerometer\ based\ estimation$.

TABLE I: Mean respiration rate (RR) and heart rate (HR) derived from accelerometer (acc), and their differences with means of the proposed methods. sb = shoulder blade, MD = mean difference, SD = standard deviation.

	RR difference (breaths/min)			HR difference (bpm)	
subject	acc	sb	centroid	acc	block
1	16.5	*-4.4*	-2.6	66.5	-3.5
2	13.4	-0.1	-0.1	50.7	-0.1
3	14.2	-1.0	-0.4	76.2	*-22.5*
4	12.7	-0.2	+0.1	61.9	-1.7
5	15.1	+0.4	-0.2	48.0	+2.2
6	12.0	-0.4	+0.3	61.3	0.0
7	11.5	-0.5	-0.3	70.4	0.0
8	12.9	*+2.0*	-2.0	57.2	-1.6
9	18.2	-0.2	+0.2	61.5	-2.5
10	16.6	+0.1	-0.2	54.2	-0.7
11	21.5	-0.2	-0.8	75.4	*-10.7*
12	12.6	-0.8	-0.4	68.9	-0.3
13	14.1	+0.1	+0.2	61.7	+5.8
14	18.5	+0.2	+0.6	61.9	+4.9
15	13.7	-1.0	-1.3	69.5	-3.5
MD		**-0.4**	**-0.5**		**-2.3**
SD		**1.3**	**0.9**		**6.7**

A. Estimation of respiration rate

The differences between the accelerometer estimation and the estimations of proposed methods are below 1.5 breaths per minute for 13 of the 15 participants. Furthermore, the

continuous estimation results of the two presented methods show good agreement with the estimation from accelerometer as shown in Fig. 4a. The mean difference of the shoulder blade method is smaller than the weighted centroid method while the maximum difference of the shoulder blade method is bigger. These differences indicate that the estimations based on the shoulder blades are slightly more accurate but also more sensitive than the estimations based on weighted centroid. The reason why the estimations are inaccurate in some measurements may be due to the contact between the torso and the PSM. Subject 1 with an inaccurate estimation has a very high BMI (31.6). Since an overweight body has a very strong contact with the PSM, both the pressure in the shoulder blade regions and the torso shape vary less during the breathing cycles compared to other participants. Subject 8 with inaccurate estimation has a different abnormal contact situation. During the whole measurement, the lower part of the torso does not have good contact with the PSM. Therefore, the amplitude of the weighted centroid vertical movement was less than other participants and irregular. Performing a linear regression on the estimations based the on shoulder blades and the estimations from accelerometer resulted in a RMSE of 1.32 with a R^2 of 0.812. Performing a linear regression on the estimations based on weighted centroid and the accelerometer resulted in a RMSE of 0.873 with a R^2 of 0.917. This shows a strong linear relationship between the estimations of the accelerometer and the proposed methods. Applying Wilcoxon rank-sum test between the mean vector of accelerometer estimation and the mean vector of the proposed methods' estimations both resulted in a failure to reject the null hypothesis at the 5% significance level (with $p - value = 0.53$ and 0.56 respectively).

B. Estimation of heart rate

An example of the continuous HR estimation is shown in Fig. 4b while the differences between the accelerometer estimations and the estimations of proposed method across all the participants are tabulated in TABLE I . The differences for HR are below 6 bpm for 13 of the 15 participants, showing a good performance in most cases. However, it remains to be investigated why the accuracy of the proposed method is poorer for some subjects.

Performing a linear regression on the estimations based on blocks and the estimations from accelerometer resulted in a RMSE of 5.55 with a R^2 of 0.6. Applying Wilcoxon rank-sum test between the mean vector of accelerometer estimation and the mean vector of the proposed method's estimations resulted in a failure to reject the null hypothesis at the 5% significance level (with $p - value = 0.38$).

V. DISCUSSION AND CONCLUSION

In this paper, we proposed novel methods to estimate the RR and the HR continuously using a PSM made by Tekscan. The results show that the performance of these methods is comparable to accelerometer based estimations. However, the performance of these methods still needs to be further investigated for more measurements with different RR, HR

values and more subjects. One limitation of the study is that due to lack of reference RR and HR measurements, we used accelerometer signals, which have been known to provide very reliable results, to compute reference values. It is necessary to repeat and further validate these experiments against true RR and HR references measured using dedicated sensors. Another limitation of the study is that the current data set is rather small. Future investigations will focus on the evaluation of subjects with varying BMI values, which was found to influence RR calculations, and subjects with higher resting HR values, which was observed to influence HR estimations. In addition, future work is needed to adapt the proposed methods in case people are non-static (i.e., data with motion artifacts) and having different lying postures (e.g. prone, or on the side).
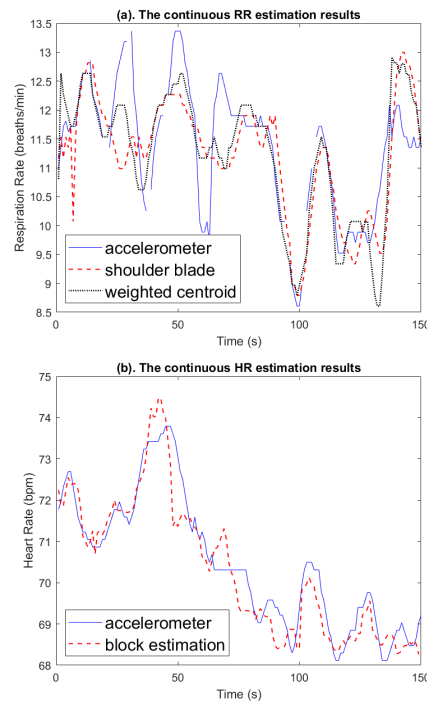
Fig. 4: Examples of RR and HR estimations from subject 7.

References

[1] M. Cretikos, R. Bellomo, K. Hillman, et al., "Respiratory rate: the neglected vital sign," Med. J. Aust., vol. 188, no. 11, pp. 657-659, 2008.

[2] A. Malhotra, and J. Loscalzo, "Sleep and cardiovascular disease: an overview," Prog. Cardiovasc. Dis., vol. 51, no. 4, pp. 279–284, 2009.

[3] L. Léger, and M. Thivierge, "Heart rate monitors: validity, stability, and functionality," Phys. Sportsmed., vol. 16, no. 5, pp. 143-151, 1988.

[4] A. M. Adami, T. L. Hayes and M. Pavel, "Unobtrusive monitoring of sleep patterns," in Proc. 25th Annu. Int. Conf. IEEE EMBS, Cancun, vol. 2, pp. 1360-1363, 2003.

[5] I. Suriani, M. Bulut, R. van Lieshout, et al., "Investigation of a ballistocardiogram-based technique for unobtrusive monitoring of fluid accumulation in the body," in 42nd Annu. Int. Conf. IEEE EMBC, Montreal, Canada, pp. 5146-5149, 2020.

[6] T. Oberlin, S. Meignen and V. Perrier, "The fourier-based synchrosqueezing transform," in 39th IEEE ICASSP, Florence, 2014, pp. 315-319.

[7] C. Lin, L. Su, and H. Wu, "Wave-shape function analysis," J. Fourier Anal. Appl. , vol. 24, pp. 451–505, 2018.